Ultrafast Dynamics of Liquid Poly(ethylene glycol)s and Crown Ethers Studied by Femtosecond Raman-Induced Kerr Effect Spectroscopy

Hideaki Shirota*

Department of General Systems Sciences, Graduate School of Arts & Sciences, University of Tokyo, 3-8-1 Komaba, Meguro-ku, Tokyo 153-8902, Japan

Received: December 24, 2004; In Final Form: February 15, 2005

Ultrafast molecular dynamics of liquid poly(ethylene glycol)s, tetra(ethylene glycol), penta(ethylene glycol), and poly(ethylene glycol) with the molecular weight of 600, and crown ethers, 12-crown-4 and 15-crown-5, have been investigated by means of femtosecond optical heterodyne-detected Raman-induced Kerr effect spectroscopy. Picosecond Kerr transients of poly(ethylene glycol)s and crown ethers are characterized by a biexponential function with the time constants of about 2 and 20 ps. Both the faster and slower time constants do not vary much among the five oligo(ethylene oxide)s. Femtosecond dynamics is discussed based on the Kerr (depolarized Raman) spectra obtained by Fourier transform deconvolution analysis of the high time resolution Kerr transients. The broad low-frequency band (0−200 cm^{-1}) in the Kerr spectrum is analyzed by two Brownian oscillators. The spectral shapes of linear poly(ethylene glycol) and cyclic crown ether are very different. Both the low- and high-frequency Brownian oscillators for crown ethers show lower frequency and broader spectral features than those for poly(ethylene glycol)s. The comparison of the low-frequency spectra of poly(ethylene glycol)s and crown ethers shows that the low-frequency spectrum of 15-crown-5 is closer to that of poly(ethylene glycol)s than that of 12-crown-4 is. The difference of the low-frequency spectra between poly(ethylene glycol) and crown ether is discussed with the concepts of molecular conformation and liquid density. The features of the observed intramolecular vibrational bands are also correlated with the molecular conformations.

1. Introduction

Polymer liquids and polymer solutions show quite distinct dynamical behaviors from simple molecular liquids and solutions.[1−5] Because of the large molecular weight and large number of constitutional repeat units, polymer dynamics occurs over a very broad time range compared with simple molecular liquids. The polymer dynamics includes the local (e.g., constitutional repeat units, segments, and side groups), entire polymer, and cooperative motions. Some fast local motions are coupled with successive slow dynamics. Nevertheless, the ultrafast dynamical aspects of polymer liquids and solutions are not well-understood yet in comparison with simple molecular liquids.

Femtosecond optically heterodyne-detected Raman-induced Kerr effect spectroscopy (OHD-RIKES) is a third-order nonlinear spectroscopy that measures the depolarized Raman signal from a transparent condensed phase in the time domain.[6,7] Several groups, especially McMorrow, Lotshaw, and coworkers, have been extensively engaged developing femtosecond OHD-RIKES in the late 1980s to the early 1990s.[6−19] The development of femtosecond OHD-RIKES was based on cw OHD-RIKES technique introduced by Levenson et al.[20,21] The femtosecond OHD-RIKES measures the dynamics in condensed phases in the time scale from 10^{-14} to 10^{-9} seconds. High quality low-frequency spectrum with the frequency range of about 0−300 cm^{-1} (depends on light pulse; about 860 cm^{-1} in this study) is available by the Fourier transform analysis of the OHD-RIKES time-domain data.[12,13] Therefore, this spectroscopy method is a powerful technique for investigating intermolecular dynamics and interactions in condensed phase. Femtosecond OHD-RIKES has been used not only for simple molecular liquids,[7,22−24] but also for complex condensed phases, such as nanoporous glasses,[25−33] microemulsions,[34−36] liquid crystals,[37−45] room-temperature ionic liquids,[46−49] aqueous peptide solutions,[50,51] and hydration protein films.[52]

Ultrafast dynamics of several polymer solutions have also been investigated by using femtosecond Kerr effect spectroscopy.[35,53−55] Sengupta, Terazima, and Fayer investigated the picosecond dynamics of poly(2-vinylnaphthalene) in CCl_4 by transient grating optical Kerr effect spectroscopy.[53] The picosecond dynamics of poly(2-vinylnaphthalene) in CCl_4 does not show the hydrodynamic behavior, while the picosecond dynamics of model monomer (2-ethylnaphthalene) in CCl_4 clearly shows the hydrodynamic behavior. They also studied poly(methylphenylsiloxane) melts.[54] Recently, we studied the femtosecond dynamics of aqueous polyacrylamide solutions by femtosecond OHD-RIKES.[55] The damped feature of the Kerr transient is very strong for aqueous polyacrylamide solutions, but aqueous propionamide solutions show much weaker damped transients than polacrylamide solutions. This difference between polymer and model-monomer solutions likely arises from the smaller contributions of diffusive reorientational and low frequency (∼40 cm^{-1}) intermolecular dynamics in polymer solutions than in model-monomer solutions. Meech and coworkers compared the ultrafast dynamics of polystyrene, oligostyrene, and bibenzyl in CCl_4.[35] The contribution of low frequency (∼50 cm^{-1}) part to the broad low-frequency spectrum

* To whom correspondence should be addressed. Present address: Department of Chemistry & Chemical Biology, Rutgers University, 610 Taylor Road, Piscataway, NJ 08854. E-mail: shirota@rutchem.rutgers.edu.

10.1021/jp044125s CCC: $30.25
Published on Web 03/19/2005

located at 0−200 cm^{-1} becomes lower with increasing the molecular weight.

One of the most fascinating synthetic polymers may be poly(ethylene oxide) (-$[CH_2CH_2O]_n$-),[56,57] because this polymer is widely used for the electrolyte support in electrochemical displays, batteries, and fuel cells.[58−62] Poly(ethylene oxide)s, oligo(ethylene oxide)s, and the derivatives are also widely used as nonionic surfactants in cosmetic, pharmaceutical, textile, and other industries.[63] In a scientific viewpoint, poly(ethylene oxide) is a very interesting polymer. For example, poly(ethylene oxide) has no side groups and shows the helical structure of the cell unit consists of the seven constitutional repeat unit in the crystal state.[64,65] Poly(ethylene oxide) is highly soluble in water and organic solvents.[66] Also, it is suggested that ion mobility in poly(ethylene oxide) is coupled with local motion of the polymer.[62]

In this paper, the ultrafast dynamics of liquid poly(ethylene glycol)s (PEGs) with the molecular weights of 194, 238, and 600 and crown ethers (CEs), 12-crown-4 and 15-crown-5, have been investigated by femtosecond OHD-RIKES. Because PEGs, the oligomers of poly(ethylene oxide), have no side groups, they are good compounds to investigate the molecular weight dependence on the fast dynamics arising from the main chain (no contribution from side groups). Furthermore, it is important to find the molecular shape effect on the dynamics by the comparison between linear and cyclic oligomers. Oligomer dynamics is of importance not only from the viewpoint of a fundamental scientific interest in molecular liquids and polymer liquids, but also because of their contribution to, or even control of, the properties of ion transportation in poly(ethylene oxide), which is of interest for use an electrolyte support. Main focus points in this study are (i) the molecular shape effect (the comparison between linear PEG and cyclic CE) and (ii) the molecular weight dependence of the ultrafast dynamics of liquid oligo(ethylene oxide)s.

2. Experimental Section

Liquid tetra(ethylene glycol) (EG4; Aldrich), penta(ethylene glycol) (EG5; Aldrich), poly(ethylene glycol) with $M_n = 600$ (PEG600; Aldrich), 12-crown-4 (CE4; Wako Pure Chemical), and 15-crown-5 (CE5; Wako Pure Chemical) were used as received. The sample liquids were injected into the sample cell with 3 mm optical path length via a 0.45 μm pore poly(tetrafluoroethylene) filter (Millipore).

The OHD-RIKES spectrometer used in this study is based on published designs,[6,13] and the details were reported elsewhere.[67] Briefly, the laser source was a lab-assembled titanium:sapphire laser, which is based on a laser kit (CDP corp., TISSA-kit-20), operating at 800 nm center wavelength (about 75 nm bandwidth) with a repetition frequency of 85 MHz, pumped by 3.5 W of 532 nm light from a Nd:VO_4 laser (Spectra Physics, Millennia Vs). The output power of the laser was about 320 mW. After the group velocity dispersion compensation by a pair of fused silica Brewster prisms, the laser beam polarization was rotated to vertical with a half wave plate and collimated by a pair of lenses. The beam was separated to pump and probe beams with an intensity ratio of 95:5 by an uncoated fused silica interferometric wedge. The pump beam was routed though a half-wave plate, a quarter-wave plate, and a Glan-Thompson polarizer set to transmit vertically polarized light. The pump beam intensity was modulated by a mechanical chopper at 1 kHz (Stanford Research Systems, SR540). The probe beam was routed through an uncoated fused silica interferometric wedge and a variable optical delay line (SIGMA TECH, FS-1050, 0.2 μm accuracy). The probe beam passed through a half-wave plate and a Glan-Thompson polarizer to set the polarization of 45 degrees from vertical, and then through a quarter-wave plate. The two beams were focused on the sample with a 150-mm focal length achromatic lens and recollimated with an identical lens. The pump beam was blocked while the probe was sent though a second Glan-Thompson polarizer (analyzer) and a spatial filter. An out of phase local oscillator was introduced by rotating the input polarizer by 1 degree away from the polarization extinction condition for heterodyne detection. A pure heterodyne Kerr signal was obtained by both the measurements of +1 and −1 degree probe input polarizer conditions. The heterodyne Kerr signal was detected by a large area amplified PIN photodiode (New Focus, 2032) and recorded by a lock-in amplifier (Stanford Research Systems, SR830). The laser pulse cross-correlation function was measured using a 200 μm KDP type-I crystal placed in the sample cell position. The response was 30 ± 3 fs fwhm (equivalent to a 19 ± 2 fs assuming a $sech^2$ pulse shape). Scans with high time resolution of 1024 points at 0.5 μm/step were recorded for a time window of 3.42 ps (10 scans for 1 transient). The slower relaxation data were captured in 80 ps scans with 25 μm/step (15 scans for 1 transient). All the measurements were made at 296 ± 2 K.

Calculations for geometry optimization and intramolecular vibrational bands of trans and gauche EG4s, CE4, and CE5 were carried out using Gaussian03 program package (Revision B. 03).[68] Density functional theory calculations were based on the Becke's three-parameter gradient-corrected exchange and Lee−Yang−Parr gradient-corrected correlation functions (B3LYP) with a basis set of 6-311+G(d,p).[69,70]

3. Data Analysis

In the OHD-RIKES experiment, the macroscopic electric polarization induced in the sample by passage of a focused femtosecond laser pulse is caused by the interaction between the third-order nonlinear molecular response and laser electric field. The Kerr response, $R(t)$, contains both an instantaneous (electronic only) hyperpolarizability contribution, $\sigma(t)$, and a sum of nuclear contributions, $r_i(t)$

$$R(t) = \sigma(t) + \sum_i r_i(t) \tag{1}$$

Because femtosecond laser pulses themselves are not instantaneous, the measured signal, $T(t)$, is a convolution of the true molecular nonlinear response with the second-order autocorrelation function of the laser pulse, $G_2(t)$

$$T(t) = \int_{-\infty}^{+\infty} G_2(t)R(\tau - t)dt \tag{2}$$

Within the bandwidth of the laser pulse, the hyperpolarizability component ($\sigma(t)$) can be separated out from the data by Fourier transform deconvolution analysis.[12,13] The nuclear dynamics in frequency domain are obtained by taking the imaginary part of the ratio of the Fourier transform of $T(t)$ and $G_2(t)$:

$$\mathrm{Im}[R(\omega)] = \mathrm{Im}\left\{\frac{F[T(t)]}{F[G_2(t)]}\right\} \tag{3}$$

The resulting frequency domain spectrum is equivalent to the low-frequency depolarized Raman spectrum times a Bose thermal occupation factor.

To obtain a sufficient number of data points for a spectrum of reasonable accuracy, it is necessary to extend the high time

resolution data over a longer time range than it is practical to record. The longer time scale Kerr transients recorded with the lower time resolution were fit to a biexponential function ($a_1 exp(-t/\tau_1) + a_2 exp(-t/\tau_2)$). The time range of 2.0−70 ps of the transients was used for fit. Prior to Fourier transform analysis, the data set was extended to 131072 points by the fit function with a time step of 3.3355 fs, yielding spectra with about 0.07624 cm^{-1}/point spacing. All the Kerr spectra obtained in this study are well resolved up to 860 cm^{-1}. The Fourier transform of the biexponential picosecond response was subtracted from the spectrum to emphasize the higher frequency intermolecular components before the line-shape analysis.

Low-frequency spectrum of 0−200 cm^{-1} frequency range for liquids contains the intermolecular dynamics. The broad feature of the low frequency spectrum in solution is essentially assigned to librational and interaction-induced intermolecular vibrational motions. Because these motions are overlapped, it is difficult to separate the contributions on low-frequency spectrum (and intermolecular dynamics).[71−75] To characterize the low-frequency Kerr spectrum in solution, several line-shape functions, such as Brownian oscillators,[76−78] Ohmic function,[17,79] sum of Ohmic and antisymmetric Gaussian functions,[80−84] and sum of Brownian oscillators and antisymmetric Gaussian function,[67] have been used to fit spectrum. Recently, McMorrow, Lotshaw and co-workers applied an inhomogeneous broadened quantum mechanical oscillator model to analyze Kerr transients of CS_2 and CS_2/isopentane.[85,86] In this study, the spectral line shape was analyzed by two Brownian oscillators:[87,88]

$$I_{BOi}(\omega) = \sum_{i=1}^{2} \frac{a_{BOi}\gamma_i\omega}{(\omega_{BOi}^2 - \omega^2)^2 + \omega^2\gamma_i^2} \quad (4)$$

where a_{BOi}, ω_{BOi}, and γ_i are the amplitude parameter, characteristic frequency, and damping constant, which is related with the friction induced by the bath on the i-th oscillator, of the i-th Brownian oscillator, respectively. The damping constant γ is assumed to be frequency independent for simplicity. Because an intramolecular band of crown ethers locates in low-frequency region (∼120 cm^{-1} for CE4 and ∼150 cm^{-1} for CE5), a Lorentzian function is added to fit the intramolecular vibrational band (see below). Sum of an Ohmic function and an antisymmetric Gaussian function did not give a better fit to the data than two Brownian oscillators model. This model fit indicates that at least two Brownian oscillators are required to fit the low-frequency Kerr spectrum in liquid oligo(ethylene oxide)s. The larger number of Brownian oscillators may be necessary, as well as simple molecular liquids.[67,76−78] However, the purpose of the fit in this study is a simple and semiquantitative representation of the low-frequency spectrum. In the case of polymers, intramolecular torsional modes also locate in the low-frequency region. The contributions of the intramolecular torsional modes to the low-frequency spectrum will be discussed in the later section.

4. Results

4.1. Picosecond Dynamics. Figure 1 shows the long time window Kerr transients of (a) PEGs, EG4 (red), EG5 (blue), and PEG600 (green), and (b) CEs, CE4 (red) and CE5 (blue). The relative amplitude of the picosecond Kerr transient signals by the nuclear responses to the electronic responses (instantaneous response at $t = 0$) for PEGs is smaller than that for CEs. All the Kerr transient data of the time range of 2−70 ps are tentatively analyzed by a biexponential function, because an exponential function and a stretched exponential function do not give a better quality fit than a biexponential function. The fit curves are also shown in Figure 1. The fit parameters are summarized in Table 1. Table 1 also lists the viscosities and densities of EG4, EG5, PEG600, CE4, and CE5.[89]

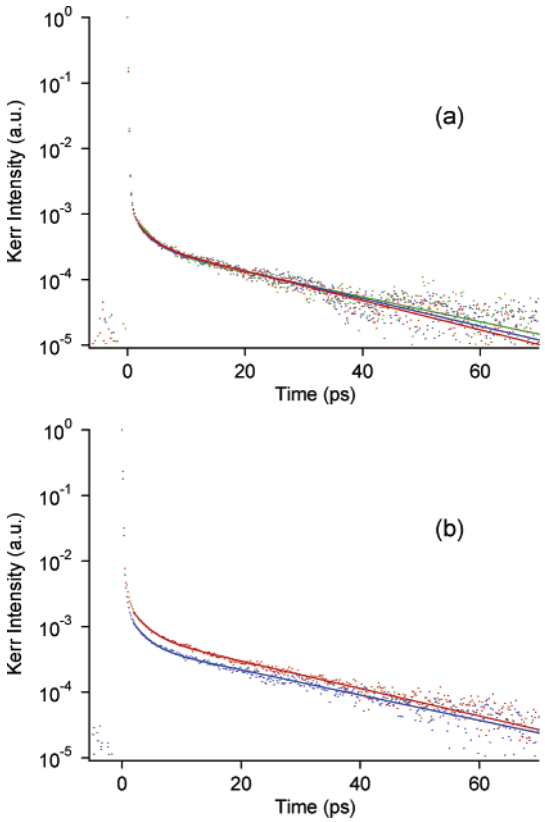

Figure 1. Long time range Kerr transients of (a) EG4 (red), EG5 (blue), and PEG600 (green) and (b) CE4 (red) and CE5(blue). Biexponential fit curves are also shown.

TABLE 1: Biexponential Fit Parameters for Picosecond Kerr Transients of Poly(ethylene glycol)s and Crown Ethers

	$a_1/(a_1+a_2)^a$	τ_1/ps^b	$a_2/(a_1+a_2)^c$	τ_2/ps^d	η/mPa·s^e	d/g mL^{-1} ^{f}
EG4	0.69	2.19	0.31	19.41	60.4	1.125
EG5	0.72	2.04	0.28	20.41	73.4	1.126
PEG600	0.76	2.57	0.24	22.90	171	1.128
CE4	0.74	2.31	0.26	20.73	12.3	1.089
CE5	0.71	2.54	0.29	23.10	30.0	1.109

[a] Fit error is ±10%. [b] Fit error is ±15%. [c] Fit error is ±10%. [d] Fit error is ±7%. [e] Values at 295 K. [f] Values at 298 K.

4.2. Femtosecond Dynamics. Figure 2 shows the high time resolution Kerr transients of (a) PEGs, EG4 (red), EG5 (blue), and PEG600 (green), and (b) CEs, CE4 (red) and CE5 (blue). The insets show the expanded time scale (0.05−0.5 ps). The high time resolution Kerr transients (Figure 2) seem to be *noisy* in comparison with the long time window transients (Figure 1). Although the number of scans for the long time window transients is larger than that for the high time resolution transients, the main origin arises from the intramolecular vibrational bands of the samples. The high time resolution transients catch the high frequency (fast time) vibrational bands for the small data spacing (3.3355 fs). In contrast, the long time window transients miss the high frequency intramolecular vibrational bands for the large data spacing (166.775 fs). The insets in Figure 2 clearly show the Kerr transients with the periodic oscillations due to the intramolecular vibrational modes. The vibrational spectra will be shown in Figure 3.

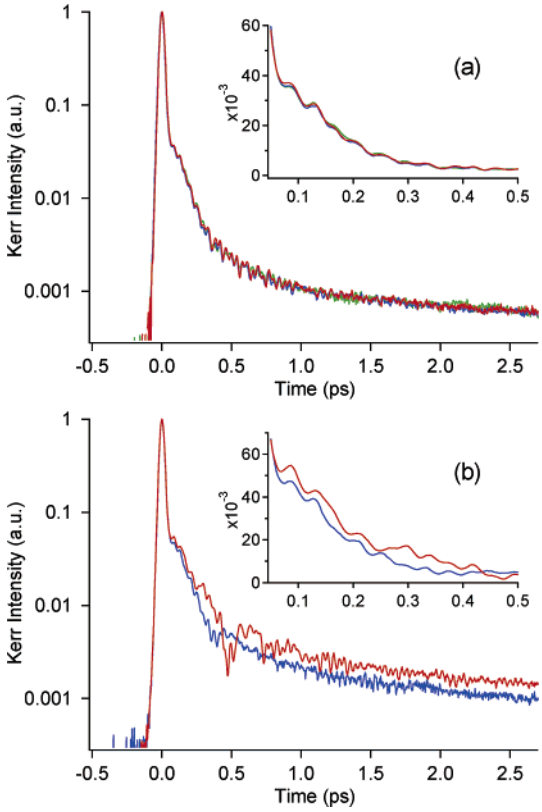

Figure 2. High time resolution Kerr transients of (a) EG4 (red), EG5 (blue), and PEG600 (green) and (b) CE4 (red) and CE5(blue). Insets show the expanded time scale (0.05−0.5 ps).

The Kerr transients of EG4, EG5, and PEG600 are almost overlapped, while the Kerr transients of CE4 and CE5 are quite different. It is also clear from the comparison between linear and cyclic oligo(ethylene oxide)s with the same number of constitutional repeat units (−CH_2CH_2O-) that the Kerr transients of oligo(ethylene oxide)s are different between linear and cyclic molecular shapes.

The high time resolution Kerr transients are analyzed by Fourier transform deconvolution procedure.[12,13] The resulting Kerr spectra subtracted the contribution of picosecond relaxation are shown in Figure 3. The notable points from Figure 3 are as follows. (1) Kerr spectra of linear PEGs (EG4, EG5, and PEG600) are different from those of cyclic CEs (CE4 and CE5). The spectrum shape of PEGs is closer to that of CE5 than that of CE4. (2) Three PEGs show quite similar spectra. (3) On the other hand, the low-frequency spectra of CE4 and CE5 are very different.

Figure 4 shows the low-frequency spectra in the frequency range of 0−200 cm^{-1} of liquid oligo(ethylene oxide)s. The fit curves by two Brownian oscillators (eq 4) are also shown in Figure 4. Although only two Brownian oscillators are used for fit, they give a good quality fit to low-frequency Kerr spectra of liquid oligo(ethylene oxide)s as shown in Figure 4. The fit parameters ω_{BOi} and γ_i and the spectral area fractions A_{BOi}, which is defined as the percentage fraction of the frequency integral of i-th Brownian oscillator per sum of the frequency integrals of two Brownian oscillators, are listed in Table 2.

4.3. Density Functional Theory Calculations. Figure 5 shows the optimized geometry structures of trans EG4, gauche EG4, CE4, and CE5 calculated by B3LYP/6-311+G(d,p) level (Cartesian coordinates for the oligo(ethylene oxide)s at the optimized geometry are summarized in Supporting Information). Because many conformations of poly(ethylene oxide) are possible, trans and gauche structures of EG4 are calculated. The trans and gauche structures are considered for all O−C−C−O units of EG4. Although EG4 takes other conformations, the two extreme structures are calculated as examples in this study. The calculated energies, mean polarizabilities α_0, and polarizability anisotropies α_{anis} are summarized in Table 3. α_0 and α_{anis} are calculated from the polarizability tensor elements α_{ij}:[90]

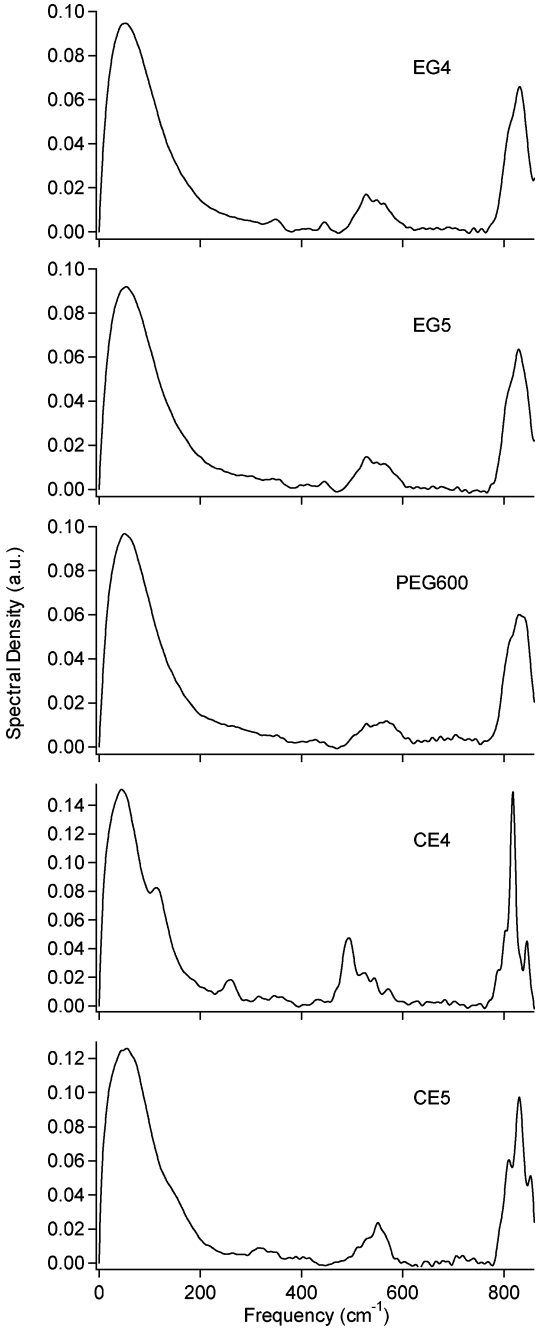

Figure 3. Fourier transform Kerr spectra of liquid EG4, EG5, PEG600, CE4, and CE5. Contribution of biexponential picosecond relaxation is subtracted.

$$\alpha_0 = \frac{\alpha_{xx} + a_{yy} + \alpha_{zz}}{3} \tag{5}$$

$$\alpha_{anis} = \sqrt{\frac{(\alpha_{xx} - \alpha_{yy})^2 + (\alpha_{yy} - \alpha_{zz})^2 + (\alpha_{zz} - \alpha_{xx})^2 + 6(\alpha_{xy}^2 + \alpha_{yz}^2 + \alpha_{zx}^2)}{2}} \tag{6}$$

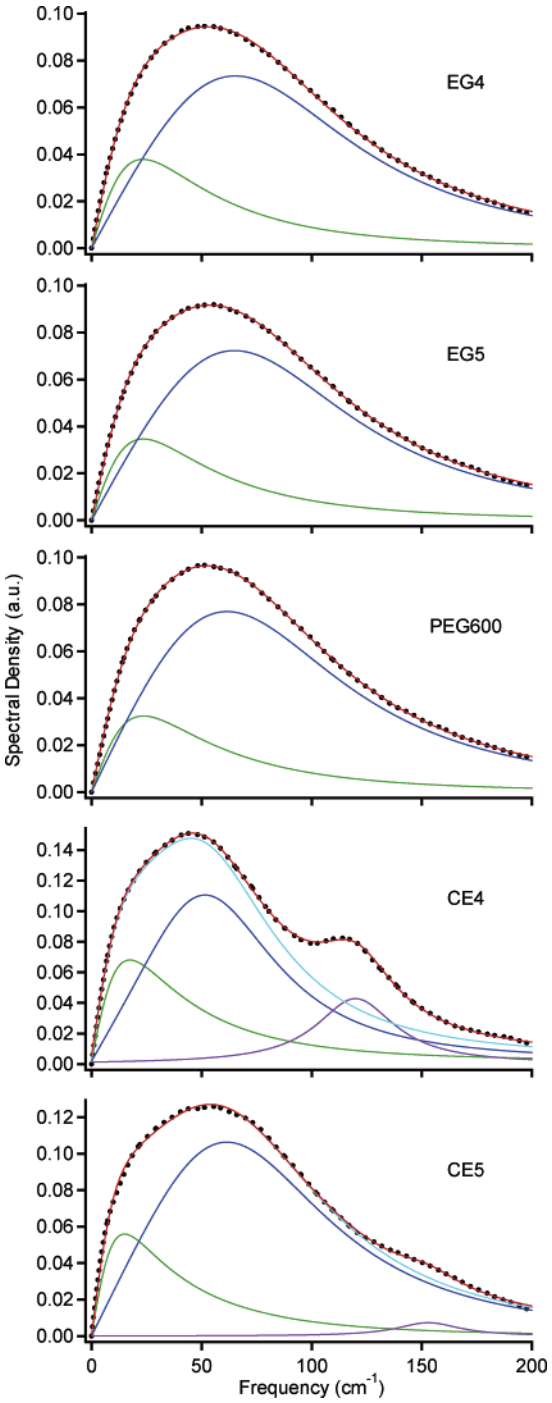

Figure 4. Fourier transform Kerr spectra with the frequency range of 0−200 cm^{-1} of oligo(ethylene oxide)s (black dotted lines). Entire fits (red lines) and two Brownian oscillators (green and blue lines) are also shown. Lorentzian fits (purple lines) for intramolecular vibrational band and sum of two Brownian oscillators (light blue lines) are also shown in CE4 and CE5.

The calculated polarizability tensor elements are summarized in Supporting Information. As shown in Table 3, trans EG4 is 5.49 kJ/mol lower than gauche EG4. The calculated Raman spectra of trans and gauche EG4s, CE4, and CE5 are shown in Figure 6. Frequency range from 0 to 900 cm^{-1} is shown in Figure 6 for an easy comparison with the Kerr spectra obtained from OHD-RIKES measurements. Calculation result of trans EG4 does not show strong intramolecular Raman-active bands in the frequency range of 750−900 cm^{-1}.

TABLE 2: Fit Parameters for Low-Frequency Kerr Spectra of Oligo(ethylene oxide)s, EG4, EG5, PEG600, CE4, and CE5

	A_{BO1}[a] (%)	ω_{BO1}[b] (cm^{-1})	γ_{BO1}[c] (cm^{-1})	A_{BO2}[d] (%)	ω_{BO2}[e] (cm^{-1})	γ_{BO2}[f] (cm^{-1})
EG4	22.4	48.4	114.4	77.6	93.5	150.5
EG5	21.5	49.2	117.3	78.5	93.1	150.0
PEG600	20.1	50.2	121.7	79.9	90.0	148.8
CE4	30.4	39.6	103.0	69.6	64.7	83.7
CE5	20.7	37.7	105.7	79.3	83.7	125.4

[a] Fit error is ±5%. [b] Fit error is ±5%. [c] Fit error is ±5%. [d] Fit error is ±4%. [e] Fit error is ±4%. [f] Fit error is ±4%.

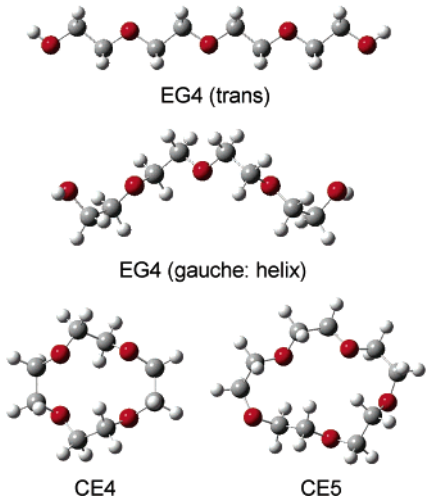

Figure 5. EG4s (trans and gauche), CE4, and CE5 at B3LYP/6-311G+(d,p) optimized geometry. White, gray, and red denote hydrogen, carbon, and oxygen, respectively.

TABLE 3: Calculated Energies, Average Polarizabilities, and Polarizability Anisotropies of EG4 (Trans and Gauche), CE4, and CE5 at B3LYP/6-311+G(d,p) Optimized Geometry

	energy (kJ/mol)	α_0 (Å^3)	α_{anis} (Å^3)
EG4 (trans)	−1816750.13	18.131	8.381
EG4 (gauche)	−1816744.64	18.328	4.069
CE4	−1615985.40	16.861	4.876
CE5	−2020004.16	21.121	5.418

5. Discussion

5.1. Picosecond Dynamics. We reported the subnanoseconds to nanosecond dynamics of PEGs and CEs studied by picosecond time-resolved fluorescence measurement using a fluorescence solvatochromic probe.[89,91] The slower nanosecond solvation time constants of liquid PEGs show a linear relationship with the molecular weight (and shear viscosity), while the faster solvation time constant of about 130 ps does not change by the different molecular weights and molecular shapes. Argaman and Huppert compared the solvation dynamics of di(ethylene glycol) dimethyl ether, tri(ethylene glycol) dimethyl ether, and tetra(ethylene glycol) dimethyl ether.[92] They showed that 10−20 ps relaxation, which is attributed to the intramolecular segmental motion, depends on the molecular weight and ∼100 ps relaxation, which is related to cooperative motions of polymers, does not vary much with the different molecular weights of oligo(ethylene glycol) dimethyl ether.

In this Kerr experiment, however, the slow nanosecond relaxation process of liquid oligo(ethylene oxide)s is not observed within the signal-to-noise ratio. As well as the present experiment, the long time scale relaxation, which includes the entire polymer motion, in polymer solutions are often missed in femtosecond Kerr experiment.[35,53,55] On the other hand, the

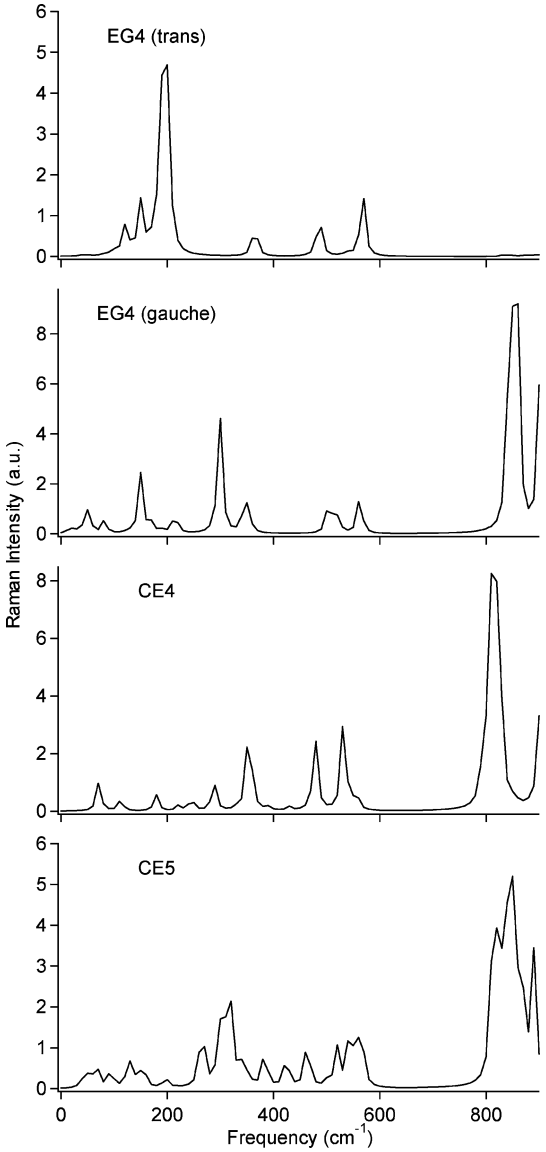

Figure 6. Calculated Raman spectra of EG4s (trans and gauche), CE4, and CE5 at B3LYP/6-311+G(d,p) optimized geometry. For a comparison with the Kerr spectra obtained by OHD-RIKES measurements, the frequency range of 0−900 cm^{-1} is shown.

slow diffusive relaxation of polymer solution is well characterized by the static and long-time pulse Kerr effect measurements. Sengupta et al. discussed this phenomenon of the missing of long time relaxation process in polymer solution measured by a femtosecond electronic field response.[53] In the static and long-time pulse Kerr effect measurements, the anisotropy relaxation of polymer solution is measured after the achievement of the dipole alignment of entire polymer along the electronic field. On the other hand, the femtosecond electronic response is too short to orient the entire polymer along the electric field. Instead, the femtosecond electronic response gives a (local) librational response of polymer. Consistently, Pecora and co-workers experimentally showed the enhancement of the amplitude of slow reorientation decay of DNA by the longer time responses.[93]

The observed Kerr relaxation time constants of EG4, EG5, PEG600, CE4 and CE5 are about 2 and 20 ps (Table 1). Both the faster and slower relaxation time constants do not show a drastic change by the variations of molecular weight and molecular shape. In simple solutions, the reorientation time is proportional to the shear viscosity (Stokes−Einstein-Debye hydrodynamic model).[94,95] Viscosity is an important factor for the relaxation time of polymer solutions.[1−5] However, the present result does not show a significant dependence of shear viscosity (and molecular weight) on the relaxation time constants.

Picosecond time scale relaxations in liquid poly(ethylene glycol)s were also reported in time-resolved fluorescence measurements,[92] dielectric relaxations,[96,97] and Brillouim scattering.[98−100] The relaxation with the time constant of 10−40 ps of PEGs is attributed to the intramolecular "crankshaft" motion (C−O−C unit reorientation).[92,97] Argaman and Huppert observed the molecular weight dependence of the solvation time for di(ethylene glycol) dimethyl ether, tri(ethylene glycol) dimethyl ether, and tetra(ethylene glycol) dimethyl ether (11.8 ps for $n = 2$, 15.4 ps for $n = 3$, and 18.2 ps for $n = 4$).[92] In contrast, Schrodle et al. observed no significant molecular weight dependence of the dielectric relaxation time constant in PEGs with $n = 1-6$ (14.3 ps for $n = 1$, 32.7 ps for $n = 2$, 18.2 ps for $n = 3$, 21.5 ps for $n = 4$, 11.1 ps for $n = 5$, and 13.5 ps for $n = 6$).[97]

The present result of Kerr relaxations for PEGs does not show a clear molecular weight dependence of the relaxation time constant of 2 ps. The time constant of cyclic CEs is also similar to that of linear PEGs. This is not surprising, because the intramolecular "crankshaft" motion is possible for both linear and cyclic oligo(ethylene oxide)s. The molecular weight dependence of the relaxation time constant shown by Argman and Huppert[92] may be reasonable in short oligo(ethylen oxide)s, such as dimer and trimer. Because the end groups can rotate freely, the intramolecular "crankshaft" motion could be affected (or coupled) by the end group reorientation. However, it may be expected that this intramolecular motion is not affected much by the end group reorientation in the case of longer PEGs.

The fast relaxation time of liquid oligo(ethylene oxide)s observed in this study is about 2 ps (Table 1). This time scale relaxation of oligo(ethylene glycol)s was also observed for dielectric relaxation[97] and solvation dynamics.[92] Schrodle et al. suggested that this relaxation could be due to the reorientation of free (no hydrogen-bonding) hydroxyl end groups. On the other hand, they also observed the similar time scale relaxation in tri(ethylene glycol) dimethyl ether, which does not have end hydroxyl groups. The present result of cyclic crown ethers also shows the relaxation with the time constant of about 2 ps. Therefore, this time scale relaxation in liquid PEGs and CEs is unlikely due to the reorientation of free hydroxyl end groups.

Argaman and Huppert attributed this time scale relaxation of oligo(ethylene oxide)s to an exponential decay memory function for non-Markovian oscillator.[92,101] In high symmetric molecular liquids, such as CS_2 and benzene, the subpicosecond intermediate exponential-like relaxation, which is slower than the femtosecond damped motions and faster than the picosecond molecular reorientation, has been treated as an intermolecular vibrational relaxation.[85,86,102,103] This quasi-exponential relaxation in simple molecular liquids is typically subpicosecond time scale. A similar relaxation likely occurs in polymer liquids. However, the time scale of the relaxation in oligo(ethylene oxide)s is slightly slower than that in simple molecular liquids.[85,86,102,103] The intermolecular vibrational relaxation process of oligo(ethylene oxide)s could be slower than that of simple molecular liquids for the large molecular weight.

5.2. Femtosecond Dynamics. *5.2.1. Intramolecular Vibrational Bands.* OHD-RIKES observes the depolarized Raman active vibrational modes. Many intramolecular vibrational bands are observed in the Fourier transform Kerr spectra of EG4, EG5, PEG600, CE4, and CE5, as shown in Figure 3. The spectra of

EG4, EG5, and PEG600 are quite similar, while the spectra of CE4 and CE5 are quite distinguishable.

It clearly finds from the comparison between the Kerr spectrum of EG4 (Figure 3) and calculated Raman spectra of trans and gauche EG4s (Figure 6) that the experimentally observed intramolecular vibrational bands (Kerr spectrum) are quite similar to the calculated Raman spectrum of gauche EG4 compared with that of trans EG4. Especially, the frequency range of 750−860 cm^{-1} is obvious. Namely, the structure of EG4 in liquid state is unlikely all-trans form. The assignments of the intramolecular vibrational bands are made based on the density functional theory calculation results and reported studies.[56,104−106] The intramolecular vibrational bands in 750−860 cm^{-1} are due to the CH_2 rocking and CO stretching modes. These intramolecular vibrational bands of PEGs are broader than those of CEs. The broad spectral feature of the intramolecular vibrational bands of PEGs arises from the conformers of the molecules. Namely, PEGs have many possible conformers, but CEs have limited conformers for the cyclic structures.

The intramolecular vibrational bands located at 450−600 cm^{-1} frequency region are C−C−O deformation and C−O−C bending modes. CE4 shows a strong vibrational mode at 493 cm^{-1}. The low-frequency intramolecular modes of CE4 (120 cm^{-1}) and CE5 (153 cm^{-1}) are C−O and C−C torsional modes. On the other hand, clear intramolecular vibrational bands of linear PEGs are absent in the low-frequency region (<200 cm^{-1}). The intensities of the torsional modes of oligo(ethylene oxide)s are weaker than those of the stretching modes (Figure 6). Furthermore, the intermolecular broad spectrum locates on this frequency region, and PEGs can take larger number of conformers than CEs. As the result, clear torsional bands of PEGs are not observed in the low-frequency region. Consistently, CE4, which is a smaller ring molecule and has smaller number of conformers, shows a clearer torsional mode than CE5, which is a larger ring molecule and has larger number of conformers. However, we note that the torsional modes of PEGs contribute on the low-frequency spectrum.

5.2.2. Broad Low-Frequency Spectrum. Broad low-frequency spectrum (dynamics) in solutions contains the both librational and interaction-induced intermolecular motions. As mentioned above, the contributions of the interaction-induced and librational motions are well overlapped in the low-frequency region (0−200 cm^{-1}).[71−75] The shape of the low-frequency spectra of linear PEGs is very different from that of cyclic CEs as shown in Figure 4. The characteristic frequencies of Brownian oscillators (ω_{BO1} and ω_{BO2}) of CEs are lower than those of PEGs, and the damping constants (γ_{BO1} and γ_{BO2}) of CEs are smaller than those of PEGs (Table 2). Furthermore, the spectral shape of CE5 is closer to that of linear PEGs than that of CE4 is.

The molecular shape of PEG is linear, and that of CE is cyclic. For the cyclic structure of CE, the degree of freedom of conformations of CE is less than that of PEG. As shown in Figure 3, the intramolecular vibrational bands of CE are shaper than those of PEG for the different degrees of freedom of conformations between CE and PEG. It may be possible that a similar effect occurs in *intermolecular* vibrational motions. Namely, increasing degree of freedom of conformations leads to the broader (more overdamped: larger γ_{BO}) spectrum for the larger inhomogeneity.

Because the intramolecular torsional modes locate in the low-frequency region (0−200 cm^{-1}) as shown in Figure 6, the intermolecular vibrations might be strongly coupled with the intramolecular torsional modes. If we compare the calculated Raman spectra of trans EG4 and gauche EG4 in the range of 0−200 cm^{-1} in Figure 6, it is clear that the different conformers yield the different frequencies of intramolecular torsional modes. The different frequency intramolecular torsional modes could lead a homogeneous broadening of the coupled intermolecular vibrational modes.

On the other hand, the liquid density may affect on the low-frequency spectrum. The liquid density of PEGs is larger than that of CEs (Table 1). The tendency of the liquid densities of the five oligo(ethylene oxide)s is $d_{PEG600} \approx d_{EG5} \approx d_{EG4} > d_{CE5} > d_{CE4}$. The concentration of the end hydroxyl groups may affect on the free volume. However, this effect is negligible small, because d_{EG4}, d_{EG5}, and d_{PEG600} are similar. Because the constitutional repeat unit is ethylene oxide for all the five oligo(ethylene oxide)s, the density difference between linear PEG and cyclic CE should be caused by the different molecular shapes. The free volumes of CE are larger than those of PEGs for the cyclic structure of CE.

Several groups reported the density dependence of the low-frequency spectrum for super critical fluids and liquids.[107−110] Low-frequency spectra of super critical fluids and liquids become broader with the higher density of fluids. The density dependence of the spectrum width of supercritical fluids is due to both homogeneous and inhomogeneous broadenings. Although the present oligo(ethylene oxide) system is larger molecular system than super critical fluids and simple liquids, a similar behavior is observed in the Kerr spectra of oligo(ethylene oxide)s as shown in Figure 4. On the other hand, the density of crystalline poly(ethylene oxide) is about 1.2 g/mL (1.169−1.239 g/mL).[111] This fact and the present result imply that the inhomogeneity for oligo(ethylene oxide)s is unlikely correlated with the liquid density.

The damping constants of PEGs are larger than those of CEs (Table 2). If we assume that the liquid density affects on the intermolecular vibrational dynamics (homogeneous broadening), the friction of an oscillator induced by the bath fractuation becomes smaller with the larger free volume (lower density) in condensed phase. As well as damping constants, the free volume could affect on the characteristic frequency of a Brownian oscillator. Because the mobile space becomes larger with the larger free volume, the displacements of intermolecular local motions, such as librational and interaction-induced intermolecular local motions, become larger with increasing the free volume. As the result, the intermolecular vibrational motions shift to the low frequency (the slow motion) for the large magnitude of displacement of the intermolecular vibrations. Surely the molecular shape difference between linear and cyclic oligo(ethylene oxide)s leads to the different liquid densities. Therefore, it is difficult to distinguish the contributions of pure molecular shape and free volume effects on the broad low-frequency spectrum in poly(ethylene oxide)s. A pressure dependence experiment might be promising to yield important information.

Although we discussed the possible origins of the intermolecular vibrational spectral boradening for PEGs compared with CEs, it is difficult to distinguish between the homogeneous and inhomogeneous broadenings of the intermolecular vibrational spectrum obtained by OHD-RIKES.[76,77] However, the present result clearly shows that the difference of the linear and cyclic structures of oligo(ethylene oxide)s provides the different low-frequency spectrum shapes, even though the oligomers have the same constitutional repeat unit.

Molecular weight dependence of oligo(ethylene oxide)s on the broad low-frequency spectrum is very different between linear and cyclic oligo(ethylene oxide)s. Three linear PEGs do

not show clear difference in the spectrum, but the spectra of CE4 and CE5 are very different. Particularly, the spectral contributions of the low and high-frequency parts (A_{BO1} and A_{BO2}) and the characteristic frequency (ω_{BO2}) and damping constant (γ_{BO2}) of the high-frequency part (second Brownian oscillator) show the large differences between PEG and CE.

The spectral contribution of the low-frequency part (first Brownian oscillator) in CE5 is smaller than that in CE4. The similar feature is observed in polymer and oligomer solutions. We showed the Kerr spectra of aqueous solutions of propionamide and polyacrylamides with the molecular weights of 1500 and 10000.[55] The spectral contribution of the low-frequency part in the broad low-frequency spectra for polyacrylamide solutions is smaller than that for propionamide solution, while no difference between polyacrylamides with the different molecular weights has been observed.[55] Aqueous solutions of some oligomers (H-[CH(COOH)CH_2]$_n$-CH_2CO_2H and H-[CH($CONH_2$)-CH_2]$_n$-CH_2CONH_2: $n = 0$, 1, and 2) show a clear n dependence on the relative contribution of the low-frequency part of the low-frequency Kerr spectra: larger n shows smaller contribution of low-frequency intermolecular mode.[112] The spectral difference between the monomer ($n = 0$) and dimer ($n = 1$) is larger than that between the dimer ($n = 1$) and trimer ($n = 2$). The spectral contribution of low-frequency part to the broad low-frequency spectrum of 1,3-diphenylpropane in CCl_4 is smaller than that of alkylbenzenzes in CCl_4.[67] If we closely see Table 2, PEGs also show a tiny trend, as well as CEs.

Both the interaction-induced and librational motions contribute on the intermolecular spectrum in simple molecular liquids.[71−75] As well as simple molecular liquids, the intermolecular vibrational motions contribute on the low-frequency spectrum in liquid oligomers and polymer solutions. As mentioned above, aqueous polyacrylamide's oligomer solutions show the molecular weight (polymerization degree) dependence of the amplitude of the low-frequency part in the broad spectrum, but polyacrylamides with the molecular weights of 1500 and 10000 are not different in the amplitude of the low-frequency spectrum.[55,112] Although the interaction-induced (and collision-induced) intermolecular translation-like motions by *entire* polymer motions are too slow to contribute in this frequency region, the librational and interaction-induced motions by the *local* polymer and oligomer motions (and solvent molecules in the case of polymer solutions) could affect on the spectrum in this low frequency range. The present result may imply that these intermolecular local motions of polymers and oligomers are less active than simple molecular liquids for the larger molecule.

The spectral shape (and parameters) of the low-frequency spectra of PEGs is closer to CE5 than CE4. This result should be due to the structural difference between CE4 and CE5. Because CE5 has a larger number of constitutional repeat unit than CE4, CE5 shows closer conformational structures (degree of freedom of conformations) and local mobility of linear PEG than CE4 does. As mentioned above, the different liquid densities (free volumes) and intramolecular torsional mode frequencies of CE4 and CE5 could also lead the different spectral features between CE4 and CE5.

6. Conclusions

In this paper, the ultrafast dynamics of liquid poly(ethylene glycol)s with the molecular weights of 194, 238, and 600 and crown ethers, 12-crown-4 and 15-crown-5, have been studied by femtosecond optically heterodyne-detected Raman-induced Kerr effect spectroscopy. The picosecond Kerr transients of liquid oligo(ethylene oxide)s have been analyzed by a biexponential function. The faster relaxation time constant is about 2 ps, and the slower relaxation time constant is about 20 ps. The faster and slower relaxations are suggested as intermolecular vibrational relaxation and intramolecular crankshaft (C−O−C) motion, respectively. Both the faster and slower relaxation time constants do not vary much among the five oligo(ethylene oxide)s. The femtosecond dynamics have been discussed based on the Fourrier transform Kerr spectra in the frequency range of 0−860 cm^{-1} obtained by Fourier transform deconvolution analysis of the high time resolution Kerr transients. The shapes of the broad low-frequency spectra (0−200 cm^{-1}) of poly(ethylene glycol)s and crown ethers are quite different. A similarity with the spectrum shape of poly(ethylene glycol)s is greater for 15-crown-5 than for 12-crown-4. The broad low-frequency spectrum has been analyzed by two Brownian oscillators. The characteristic frequencies and damping constants of both low- and high-frequency Brownian oscillators for crown ethers are lower than those for poly(ethylene glycol)s. This spectral difference between linear poly(ethylene glycol) and cyclic crown ether should be due to the different degrees of freedom of conformations and/or different free volumes arising from the molecular shape difference. Because the cyclic structure of 12-crown-4 is more constrained than 15-crown-5 for the smaller number of constitutional repeat units, the spectral feature of 12-crown-4 is more distinguishable from that of poly(ethylene glycol)s than that of 15-crown-5 is. The intramolecular vibrational bands of 12-crown-4 are also very different from those of poly(ethylene glycol)s. The relative contribution (spectral area) of the low-frequency part (low-frequency Brownian oscillator) to the high-frequency part (high-frequency Brownian oscillator) in the broad low-frequency spectrum (0−200 cm^{-1}) becomes smaller with increasing molecular weight, as well as other oligomers and polymers in solutions.

Acknowledgment. Professor Ken-ichi Saitow (Hiroshima University) is thanked for helpful discussion and suggestion of informative references. This work was partially supported by the Yamada Science Foundation and the Ministry of Education, Culture, Sports, Science and Technology of Japan (Grant No. 15750097 and the 21st Century COE program: Research Center for Integrated Science).

Supporting Information Available: Additional experimental details. This material is available free of charge via the Internet at http://pubs.acs.org.

References and Notes

(1) Flory, P. J. *Principles of Polymer Chemistry*; Cornell University Press: Ithaca, 1953.

(2) de Gennes, P. D. *Scaling Concepts in Polymer Physics*; Cornell University Press: Ithaca, 1979.

(3) Doi, M.; Edwards, S. F. *The Theory of Polymer Dynamics*; Oxford University Press: Oxford, 1986.

(4) Matsuoka, S. *Relaxation Phenomena in Polymers*; Carl Hanser Verlag: Munich, 1992.

(5) Strobl, G. R. *The Physics of Polymers*, 2nd ed.; Springer: Berlin, 1997.

(6) McMorrow, D.; Lotshaw, W. T.; Kenney-Wallace, G. A. *IEEE J. Quantum Electron.* **1988**, *24*, 443.

(7) Lotshaw, W. T.; McMorrow, D.; Thantu, N.; Melinger, J. S.; Kitchenham, R. *J. Raman Spectrosc.* **1995**, *26*, 571.

(8) Lotshaw, W. T.; McMorrow, D.; Kalpouzos, C.; Kenney-Wallace, G. A. *Chem. Phys. Lett.* **1987**, *136*, 323.

(9) Kalpouzos, C.; Lotshaw, W. T.; McMorrow, D.; Kenney-Wallace, G. A. *J. Phys. Chem.* **1987**, *91*, 2028.
(10) Kalpouzos, C.; McMorrow, D.; Lotshaw, W. T.; Kenney-Wallace, G. A. *Chem. Phys. Lett.* **1988**, *150*, 138.
(11) Kalpouzos, C.; McMorrow, D.; Lotshaw, W. T.; Kenney-Wallace, G. A. *Chem. Phys. Lett.* **1989**, *155*, 240.
(12) McMorrow, D.; Lotshaw, W. T. *Chem. Phys. Lett.* **1990**, *174*, 85.
(13) McMorrow, D.; Lotshaw, W. T. *J. Phys. Chem.* **1991**, *95*, 10395.
(14) McMorrow, D.; Lotshaw, W. T. *Chem. Phys. Lett.* **1991**, *178*, 69.
(15) Hattori, T.; Kobayashi, T. *J. Chem. Phys.* **1991**, *94*, 7289.
(16) Wynne, K.; Galli, C.; Hochstrasser, R. M. *Chem. Phys. Lett.* **1992**, *193*, 17.
(17) Cho, M.; Du, M.; Scherer, N. F.; Fleming, G. R.; Mukamel, S. *J. Chem. Phys.* **1993**, *99*, 2410.
(18) Chang, Y. J.; Castner, E. W., Jr. *J. Chem. Phys.* **1993**, *99*, 7289.
(19) Chang, Y. J.; Castner, E. W., Jr. *J. Chem. Phys.* **1993**, *99*, 113.
(20) Eesley, G. L.; Levenson, M. D.; Tolles, W. M. *IEEE J. Quantum Electron.* **1978**, *QE−14*, 45.
(21) Levenson, M. D.; Eesley, G. L. *Appl. Phys.* **1978**, *19*, 1.
(22) Kinoshita, S.; Kai, Y.; Ariyoshi, T.; Shimada, Y. *Int. J. Mod. Phys. B* **1996**, *10*, 1229.
(23) Castner, E. W., Jr.; Maroncelli, M. *J. Mol. Liq.* **1998**, *77*, 1.
(24) Smith, N. A.; Meech, S. R. *Int. Rev. Phys. Chem.* **2002**, *21*, 75.
(25) Loughnane, B. J.; Farrer, R. A.; Scodinu, A.; Reilly, T.; Fourkas, J. T. *J. Phys. Chem. B* **2000**, *104*, 5421.
(26) Farrer, R. A.; Fourkas, J. T. *Acc. Chem. Res.* **2003**, *36*, 605.
(27) Loughnane, B. J.; Fourkas, J. T. *J. Phys. Chem. B* **1998**, *102*, 10288.
(28) Loughnane, B. J.; Farrer, R. A.; Fourkas, J. T. *J. Phys. Chem. B* **1998**, *102*, 5409.
(29) Loughnane, B. J.; Farrer, R. A.; Scodinu, A.; Fourkas, J. T. *J. Chem. Phys.* **1999**, *111*, 5116.
(30) Loughnane, B. J.; Scodinu, A.; Fourkas, J. T. *J. Phys. Chem. B* **1999**, *103*, 6061.
(31) Loughnane, B. J.; Scodinu, A.; Fourkas, J. T. *Chem. Phys.* **2000**, *253*, 323.
(32) Scodinu, A.; Fourkas, J. T. *J. Phys. Chem. B* **2002**, *106*, 10292.
(33) Scodinu, A.; Farrer, R. A.; Fourkas, J. T. *J. Phys. Chem. B* **2002**, *106*, 12863.
(34) Hunt, N. T.; Jaye, A. A.; Meech, S. R. *J. Phys. Chem. B* **2003**, *107*, 3405.
(35) Hunt, N. T.; Jaye, A. A.; Hellman, A.; Meech, S. R. *J. Phys. Chem. B* **2004**, *108*, 100.
(36) Jaye, A. A.; Hunt, N. T.; Meech, S. R. *Langmuir* **2005**, *21*, 1238.
(37) Stankus, J. J.; Torre, R.; Marshall, C. D.; Greenfield, S. R.; Sengupta, A.; Tokmakoff, A.; Fayer, M. D. *Chem. Phys. Lett.* **1992**, *194*, 213.
(38) Stankus, J. J.; Trroe, R.; Fayer, M. D. *J. Phys. Chem.* **1993**, *97*, 9478.
(39) Gottke, S. D.; Brace, D. D.; Cang, H.; Bagchi, B.; Fayer, M. D. *J. Chem. Phys.* **2002**, *116*, 360.
(40) Gottke, S. D.; Cang, H.; Bagchi, B.; Fayer, M. D. *J. Chem. Phys.* **2002**, *116*, 6339.
(41) Cang, H.; Li, H.; Fayer, M. D. *Chem. Phys. Lett.* **2002**, *366*, 82.
(42) Cang, H.; Li, J.; Novikov, V. N.; Fayer, M. D. *J. Chem. Phys.* **2003**, *119*, 10421.
(43) Hyun, B. R.; Quitevis, E. L. *Chem. Phys. Lett.* **2003**, *373*, 526.
(44) Hyun, B. R.; Quitevis, E. L. *Chem. Phys. Lett.* **2003**, *370*, 725.
(45) Hunt, N. T.; Meech, S. R. *J. Chem. Phys.* **2004**, *120*, 10828.
(46) Hyun, B. R.; Dzyuba, S. V.; Bartsch, R. A.; Quitevis, E. L. *J. Phys. Chem. A* **2002**, *106*, 7579.
(47) Rajian, J. R.; Li, S.; Bartsch, R. A.; Quitevis, E. L. *Chem. Phys. Lett.* **2004**, *393*, 372.
(48) Cang, H.; Li, J.; Fayer, M. D. *J. Chem. Phys.* **2003**, *119*, 13017.
(49) Giraud, G.; Gordon, C. M.; Dunkin, I. R.; Wynne, K. *J. Chem. Phys.* **2003**, *119*, 464.
(50) Giraud, G.; Wynne, K. *J. Am. Chem. Soc.* **2002**, *124*, 12110.
(51) Giraud, G.; Karolin, J.; Wynne, K. *Biophys. J.* **2003**, *85*, 1903.
(52) Eaves, J. D.; Fecko, C. J.; Stevens, A. L.; Peng, P.; Tokmakoff, A. *Chem. Phys. Lett.* **2003**, *376*, 20.
(53) Sengupta, A.; Terazima, M.; Fayer, M. D. *J. Phys. Chem.* **1992**, *96*, 8619.
(54) Sengupta, A.; Fayer, M. D. *J. Chem. Phys.* **1994**, *100*, 1673.
(55) Shirota, H.; Castner, E. W., Jr. *J. Am. Chem. Soc.* **2001**, *123*, 12877.
(56) Bailey, F. E., Jr.; Koleske, J. V. *Poly(ethylene oxide)*; Academic Press: New York, 1976.
(57) *Poly(ethylene glycol): Chemistry and Biological Applications*; Harris, J. M., Zalipsky, S., Eds.; American Chemical Society: Washington, DC, 1997; Vol. 680.
(58) Armand, M. B. *Annu. Rev. Mater. Sci.* **1986**, *4*, 245.
(59) Ratner, M. A.; Shriver, D. F. *Chem. Rev.* **1988**, *88*, 109.
(60) Watanabe, M.; Ogata, N. *Brit. Polym. J.* **1988**, *20*, 181.
(61) Wright, P. V. *J. Macromol. Sci. A* **1989**, *26*, 519.
(62) Bruce, P. G.; Vincent, C. A. *J. Chem. Soc., Faraday Trans.* **1993**, *89*, 3187.
(63) *Nonionic Surfactants*; Schick, M. J., Ed.; Marcel Dekker: New York, 1967.
(64) Takahashi, Y.; Tadokoro, H. *Macromolecules* **1973**, *6*, 672.
(65) Russell, T. P.; Ito, H. *Macromolecules* **1988**, *21*, 1703.
(66) Saeki, S.; Kuwahara, N.; Nakata, M.; Kaneko, M. *Polymer* **1976**, *17*, 685.
(67) Shirota, H. *J. Chem. Phys.* **2005**, *122*, 044514.
(68) Frisch, M. J.; Trucks, G. W.; Schlegel, H. B.; Scuseria, G. E.; Robb, M. A.; Cheeseman, J. R.; Montgomery, J. A., Jr.; Vreven, T.; Kudin, K. N.; Burant, J. C.; Millam, J. M.; Iyengar, S. S.; Tomasi, J.; Barone, V.; Mennucci, B.; Cossi, M.; Scalmani, G.; Rega, N.; Petersson, G. A.; Nakatsuji, H.; Hada, M.; Ehara, M.; Toyota, K.; Fukuda, R.; Hasegawa, J.; Ishida, M.; Nakajima, T.; Honda, Y.; Kitao, O.; Nakai, H.; Klene, M.; Li, X.; Knox, J. E.; Hratchian, H. P.; Cross, J. B.; Adamo, C.; Jaramillo, J.; Gomperts, R.; Stratmann, R. E.; Yazyev, O.; Austin, A. J.; Cammi, R.; Pomelli, C.; Ochterski, J. W.; Ayala, P. Y.; Morokuma, K.; Voth, G. A.; Salvador, P.; Dannenberg, J. J.; Zakrzewski, V. G.; Dapprich, S.; Daniels, A. D.; Strain, M. C.; Farkas, O.; Malick, D. K.; Rabuck, A. D.; Raghavachari, K.; Foresman, J. B.; Ortiz, J. V.; Cui, Q.; Baboul, A. G.; Clifford, S.; Cioslowski, J.; Stefanov, B. B.; Liu, G.; Liashenko, A.; Piskorz, P.; Komaromi, I.; Martin, R. L.; Fox, D. J.; Keith, T.; Al-Laham, M. A.; Peng, C. Y.; Nanayakkara, A.; Challacombe, M.; Gill, P. M. W.; Johnson, B.; Chen, W.; Wong, M. W.; Gonzalez, C.; Pople, J. A. *Gaussian 03*, Gaussian, Inc.: Pittsburgh, PA, 2003.
(69) Becke, A. D. *J. Chem. Phys.* **1993**, *98*, 5648.
(70) Lee, C.; Yang, W.; Parr, R. G. *Phys. Rev. B* **1988**, *37*, 785.
(71) Madden, P. A.; Cox, T. I. *Mol. Phys.* **1981**, *43*, 287.
(72) Madden, P. A. In *Ultrafast Phenomena IV*; Auston, A. H., Eisenthal, K. B., Eds.; Springer-Verlag: Berlin, 1984; p 244.
(73) Geiger, L. C.; Ladanyi, B. M. *J. Chem. Phys.* **1988**, *89*, 6588.
(74) Geiger, L. C.; Ladanyi, B. M. *Chem. Phys. Lett.* **1989**, *159*, 413.
(75) Ryu, S.; Stratt, R. M. *J. Phys. Chem. B* **2004**, *108*, 6782.
(76) Palese, S.; Buontempo, J. T.; Schlling, L.; Lotshaw, W. T.; Tamimura, Y.; Mukamel, S.; Dwayne Miller, R. J. *J. Phys. Chem.* **1994**, *98*, 12466.
(77) Palese, S.; Mukamel, S.; Dwayne Miller, R. J.; Lotshaw, W. T. *J. Phys. Chem.* **1996**, *100*, 10380.
(78) Bartolini, P.; Ricci, M.; Torre, R.; Righini, R.; Santa, I. *J. Chem. Phys.* **1999**, *110*, 8653.
(79) Shirota, H.; Yoshihara, K.; Smith, N. A.; Lin, S.; Meech, S. R. *Chem. Phys. Lett.* **1997**, *281*, 27.
(80) Chang, Y. J.; Castner, E. W., Jr. *J. Phys. Chem.* **1994**, *98*, 9712.
(81) Chang, Y. J.; Castner, E. W., Jr. *J. Phys. Chem.* **1996**, *100*, 3330.
(82) Smith, N. A.; Lin, S.; Meech, S. R.; Shirota, H.; Yoshihara, K. *J. Phys. Chem. A* **1997**, *101*, 9578.
(83) Smith, N. A.; Lin, S.; Meech, S. R.; Yoshihara, K. *J. Phys. Chem. A* **1997**, *101*, 3641.
(84) Smith, N. A.; Meech, S. R. *J. Phys. Chem. A* **2000**, *104*, 4223.
(85) McMorrow, D.; Thantu, N.; Kleiman, V.; Melinger, J. S.; Lotshaw, W. T. *J. Phys. Chem. A* **2001**, *105*, 7960.
(86) McMorrow, D.; Lotshaw, W. T.; Melinger, J. S.; Kleiman, V. *ACS Symp. Ser.* **2002**, *820*, 14.
(87) Tanimura, Y.; Mukamel, S. *J. Chem. Phys.* **1993**, *99*, 9496.
(88) Mukamel, S. *Principles of Nonlinear Optical Spectroscopy*; Oxford University Press: New York, 1995.
(89) Shirota, H.; Segawa, H. *J. Phys. Chem. A* **2003**, *107*, 3719.
(90) Long, D. A. *The Raman Effect*; John Wiley & Sons: West Sussex, 2002.
(91) Shirota, H.; Segawa, H. *Chem. Phys.* **2004**, *306*, 43.
(92) Argaman, R.; Huppert, D. *J. Phys. Chem. A* **1998**, *102*, 6215.
(93) Lewis, R. J.; Pecora, R.; Eden, D. *Macromolecules* **1986**, *19*, 134.
(94) Dote, J. L.; Kivelson, D.; Schwartz, R. N. *J. Phys. Chem.* **1981**, *85*, 2169.
(95) Fleming, G. R. *Chemical Applications of Ultrafast Spectroscopy*; Oxford University Press: New York, 1986.
(96) Kaatze, U.; Kettler, M.; Pottel, R. *J. Phys. Chem.* **1996**, *100*, 2360.
(97) Schrodle, S.; Buchner, R.; Kunz, W. *J. Phys. Chem. B* **2004**, *108*, 6281.
(98) Wang, C. H.; Lin, Y.-H.; Jones, D. R. *Mol. Phys.* **1979**, *37*, 287.
(99) Wang, C. H.; Li, B. Y.; Rendell, R. W.; Ngai, K. L. *J. Non-Crystal. Solids* **1991**, *131−133*, 870.
(100) Noudou, T.; Matsuoka, T.; Koda, S.; Nomura, H. *Jpn. J. Appl. Phys.* **1996**, *35*, 2944.
(101) Fainberg, B. D.; Huppert, D. *J. Mol. Liq.* **1995**, *64*, 123.
(102) Loughnane, B. J.; Scodinu, A.; Farrer, R. A.; Fourkas, J. T.; Mohanty, U. *J. Chem. Phys.* **1999**, *111*, 2686.
(103) Scodinu, A.; Fourkas, J. T. *J. Phys. Chem. B* **2003**, *107*, 44.
(104) Koenig, J. L.; Angood, A. C. *J. Polym. Sci., Part A-2* **1970**, *8*, 1787.

(105) Matsuura, H.; Fukuhara, K. *J. Mol. Struct.* **1985**, *126*, 251.
(106) Fukuhara, K.; Ikeda, K.; Matsuura, H. *J. Mol. Struct.* **1990**, *224*, 203.
(107) Gerschel, A.; Dimicoli, I.; Jaffre, J.; Riou, A. *Mol. Phys.* **1976**, *32*, 679.
(108) Bohn, M. A.; Franck, E. U. *Ber. Bunsen-Ges. Phys. Chem.* **1988**, *92*, 850.
(109) Saitow, K.; Ohtake, H.; Sarukura, N.; Nishikawa, K. *Chem. Phys. Lett.* **2001**, *341*, 86.
(110) Song, W.; Patel, N.; Maroncelli, M. *J. Phys. Chem. B* **2002**, *106*, 8783.
(111) *Polymer Handbook*, 4th ed.; Brandrup, J., Inmergut, E. H., Grulke, E. A., Eds.; John Wiley & Sons: New York, 1999.
(112) Shirota, H.; Ushiyama, H. Manuscript in preparation.